J-SuNR

JOURNAL OF SUSTAINABLE NATURAL RESOURCES
e-ISSN: 2716-7143

Vol. 7 No. 1 (2026) 34-46
https://publisher.uthm.edu.my/ojs/index.php/j-sunr

Geophysical and GIS Model for Assessment of Groundwater Vulnerability in Owa-Kajola Marble Mining Site, Southwestern Nigeria

Kehinde Olojoku Ibrahim[1]*, Rukayat Tolulope Ayanlere[1], Umar Faruk Aliyu[1], Azeez Adewale Adejumo[2], Abdulwahid Kolawole Aweda[3]

[1] *Department of Geology and Mineral Sciences, University of Ilorin, NIGERIA*
[2] *Environmental Science and Policy, Pace University, New York, UNITED STATES*
[3] *Department of Geology and Mining, Ibrahim Badamasi Babangida University Lapai, Lapai, NIGERIA*

*Corresponding Author: ibrahim.ko@unilorin.edu.ng
DOI: https://doi.org/10.30880/jsunr.2026.07.01.004

Article Info

Received: 24 October 2025
Accepted: 9 June 2026
Available online: 30 June 2026

Keywords

Mining, marble, groundwater, geophysical, GIS, vulnerability

Abstract

Despite the economic impact of mining, its negative effects on the environment require an assessment and urgent solution for environmental restoration. The aim of this study was to determine spatial distribution of groundwater vulnerability in Owa-Kajola marble mining site, Southwestern Nigeria using geophysical and GIS model. Vertical electrical sounding (VES) using Schlumberger arrangement was carried out in ten (10) locations. Five (5) geoelectric layers are recognised which include top soil, clay-sandy, sand-clayey, weathered, and fresh basements. Generated curve distributions are QH, HA and H curve types respectively. The first top layer has resistivity values between 82Ωm to 987Ωm, thickness of 0.1m to 1.6m, and depth between 0.1m to 1.6m. The second layer is clay-sandy with values ranges between 84Ωm to 389Ωm, thickness of 0.2m to 9.2m, depth between 0.3m to 10.8m. Third geoelectric layer is sand-clayey with values between 18Ωm to 125Ωm, thickness of 2m to 6.2m and depth of 2.7m to 9.6m, fourth geoelectric layer is weathered basement with values of 19Ωm to 1145Ωm, thickness of 0.5m to 50m and depth of 0.8m to 57.3m while the fifth geoelectric layer is fresh basement with resistivity values ranges between 34Ωm to 2847Ωm. Estimated aquifer protective capacity revealed that study area has aquifer protective capacity values between 0.00 and 0.69 with moderate zones (30%), weak zone (10%) and poor zones (60%). The moderate zones have values range from 0.23 to 0.69, covering the northern to eastern parts of the area. The weak zone has value of 0.17 in eastern parts while poor zones dominate the western to southern parts with values between 0.00 to 0.01 respectively, thus indicating that most parts of the area are poorly protected and prone to groundwater contamination. ArcGIS software (version 10.8.2) was used to generate groundwater vulnerability maps. This study shows that geophysical methods and GIS model are effective tools for groundwater vulnerability assessment. The study recommended continuous monitoring of groundwater and seek for control of mining activities to protect groundwater resources.

1. Introduction

Groundwater is used as a source of drinking water in the majority of cities across the world [1]. More than 50% of the world population rely on groundwater for drinking, domestic and agricultural purposes [2]. The reliance on groundwater resource demands that water occurrence within the subsurface is of significant quantity and quality [3]. Mining natural resources, including metallic and non-metallic minerals as well as fossil fuels like coal, natural gas, and petroleum is crucial to a country's economic growth because it creates jobs in the public and private sectors and increases foreign exchange [4]. However, several detrimental effects on the ecosystem have been linked to mining operations [5]. Mining activities produce some toxic metals that can be injurious to humans. For instance, approximately about 40% of marble waste is generated globally during quarrying operations. This waste can take the form of rock fragments that are then disposed of in landfills, nearby empty pits, roads, riverbeds, pasture lands, agricultural fields, or other locations, causing environmental and groundwater pollution to spread widely. Groundwater vulnerability study is an essential tool in environmental pollution assessment and control. Efforts have been made by hydrogeologists, hydrologists, water engineers and environmentalists to protect groundwater against pollution and contamination [6]. This led to the development of different methods for groundwater vulnerability assessments. These vulnerability methods include GOD [7], AVI [8], DRASTIC [9], SINTACS [10], among others. Geophysical and geographical information system (GIS) methods have been used for effective delineation of aquifer protective capacity [11]. Geophysical method such as electrical resistivity method is very important to know the lithology, aquifer properties and assessment of groundwater vulnerability [12]. Few studies have been carried out in study area which include geochemical assessment of marble for cement production [13] and health risk assessment of trace elements [14]. However, assessment of groundwater vulnerability has not been reported in the study area. This study was carried out to integrate geoelectrical data and produce a spatial distribution map of groundwater vulnerability in study area.

2. Study Area

The study area (Owa-Kajola) and its environs fall between N8^0 02'07'' to N8^0 04'36'' and E5^0 01'13''to E5^0 02'28'' (Figure 1). The area is a northern continuation of the Ilesha Schist Belt [15]. It is essentially a Precambrian suite of intensely deformed metasediments which occupy a linear belt underlain by rock of migmatite gneiss, amphibolite, calc-silicate gneiss, mica schist, quartzite (member of the Omu-Aran Dyon Hills), pegmatite of Precambrian age and marble (Figure 2). The lenticular marble deposit occurs in the study area (Figure 3) and is well exposed about two kilometers south of Kajola to the east of a major quartzite hill. Groundwater in the area is positioned in wide weathered zones and fractures that are mostly replenished by rainwater.

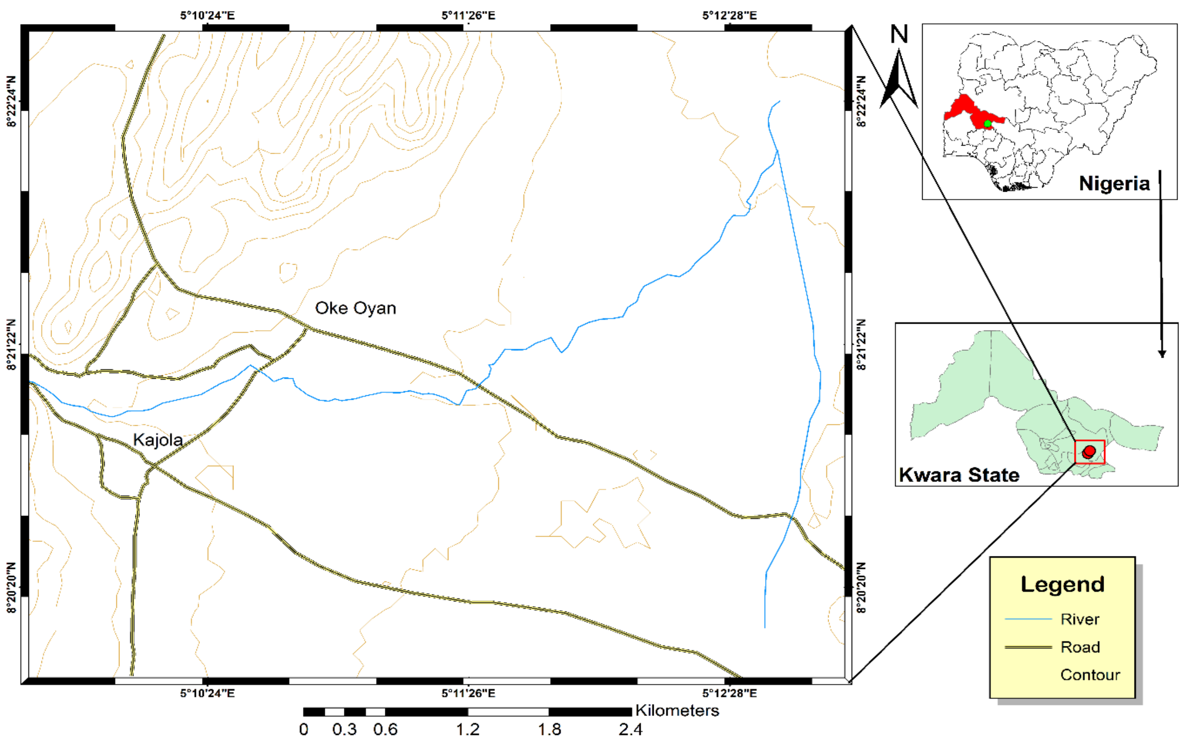

Fig. 1 *Location of the study area*

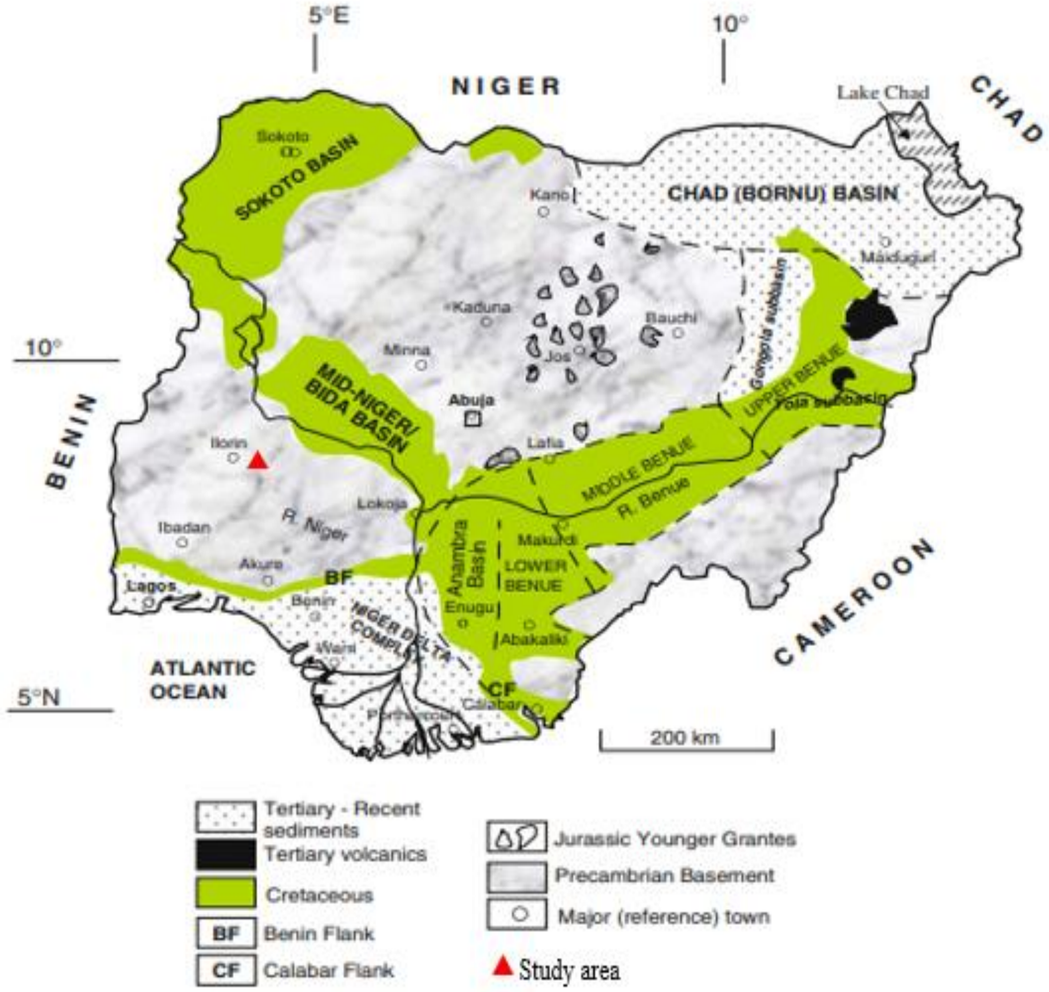

Fig. 2 *Geological map of Nigeria showing study area*

Fig. 3 *Sparkling white marble lumps ready for haulage in study area*

3. Materials and Methods

Geoelectrical characteristics, subsurface lithology, and spatial distribution of groundwater vulnerability in study area were determined by electrical resistivity sounding (VES) using Schlumberger array and geographic information system (GIS) in ten (10) locations (Figure 4). Schlumberger array was used due to its higher accuracy, better vertical resolution and provides greater depth of investigation. Four (4) electrodes were placed in a straight line for the field sounding exercise (Figure 4).

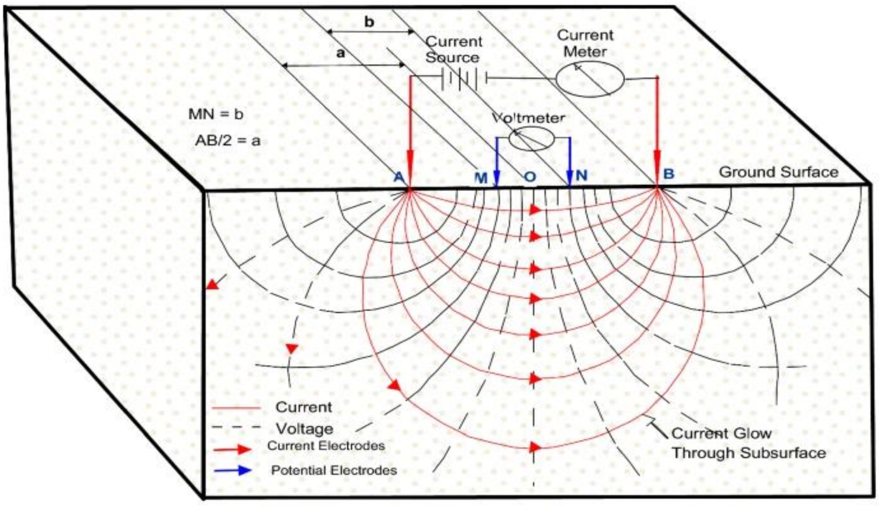

Fig. 4 *Schematic diagram of electrical resistivity operating principles [15]*

The potential and current electrodes were not positioned equally apart, two current electrodes, A and B, and two potential electrodes, M and N, were positioned in line with one another and centered on specific spots (Figure 4) while potential electrodes were utilized to quantitatively measure the voltage system on the surface resulting from the current flow patterns by the first set of electrodes, current was transferred into the ground by current electrodes. From the principle of Ohm's law given as follows:

$$R = \frac{V}{I} \tag{1}$$

Where,
R = resistance, measured in ohms (Ω)
V = voltage (or potential difference, measured in volts (V)
I = electrical current, measured in amperes

$$\rho_\alpha = KR \tag{2}$$

Where,
ρ_α = apparent resistivity
K = geometric factor
R = measured resistance

$$R = \rho\frac{L}{A} = V = I\rho\frac{L}{A} \tag{3}$$

Where,
R = resistance, measured in ohms (Ω)
ρ = apparent resistivity
L = Length of conductor (in meters)
A = cross-sectional area of the conductor (in square meters)

A resistivity meter MODEL SSR MP1 was used to generate resistivity data. The maximum spreads for AB/2 and MN/2 are 160m and 7.5m respectively. *Ra* is apparent electrical resistance and determined from resistivity meter.

$$p_a = n \times \left[\frac{\left(\frac{AB}{2}\right)^2 - \left(\frac{MN}{2}\right)^2}{MN} \right] \times R_a \tag{4}$$

The resistivity meter's apparent electrical resistance (*Ra)* is distance between the two current electrodes (*AB*) and the potential electrodes (*MN*). Also, the equation (4) above is written as:

$$\rho_\alpha = K \times R_\alpha \tag{5}$$

Where K is the geometrical factor:

$$K = n \times \left[\frac{\left(\frac{AB}{2}\right)^2 - \left(\frac{MN}{2}\right)^2}{MN} \right] \tag{6}$$

The VES curves were generated through the plotting of apparent resistivity (ρa) on a bi-logarithm graph against the matching half electrode separation (*AB/2*). Partial curve matching was used to analyze sounding curves, providing the resistivity of the layers with thicknesses. IPI2 WIN software was used to invert the results.

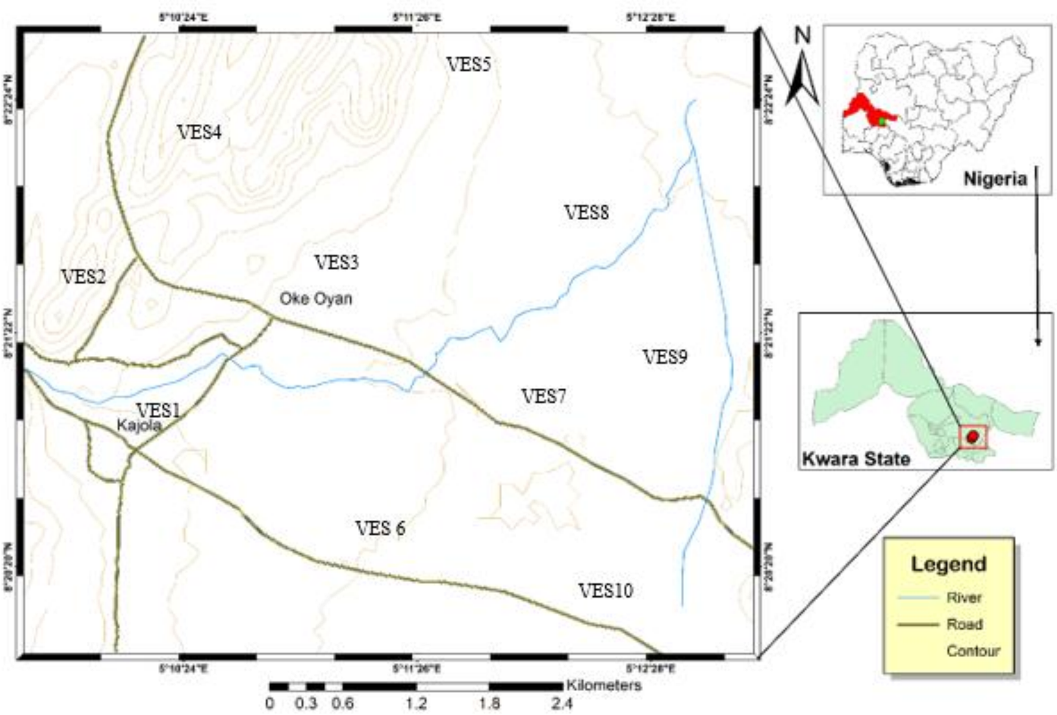

Fig. 5 *Map showing VES locations*

3.1 Aquifer Protective Capacity and Groundwater Vulnerability Assessment

Aquifer vulnerability is a measure of the rate at which the overburden layers of an aquifer formation can impede or allow the flow of contaminant to the aquifer. It is the summation of the ratio of the thickness of overburden formations to their resistivities [16]. Aquifer vulnerability determines whether the sub-surface's physical and chemical properties will favour or inhibit the penetration of harmful compounds from the earth's surface, which could jeopardize the quality of groundwater. Percolating fluids are thought to be naturally filtered by the earth's subsoil. Therefore, a measure of its protective capacity refers to its ability to filter and retard any percolating fluid [17].

The term Dar-Zarrouk on electrical prospecting was introduced by [18] for describing a relationship between the longitudinal unit conductance (*S*) in mho and transverse resistance (*R*) in Ωm^2 which are used for evaluation of aquifer hydraulic parameters and protective capacity of the overburden rock materials [19]. These parameters are based on the analogy between groundwater and electrical current flow [20]. The underlying aquifer is protected by impermeable rock material that possess high longitudinal conductivity. The protective property is derived from aquifer longitudinal conductance (Table 1), both of which are determined by the aquifer thickness (h_i) and apparent resistivity (ρ_i) based on Dar-Zarrouk principle. The parameters can be determined using the equations (7) and (8):

$$Si = \frac{hi}{\rho i} = \sum_{i=1}^{n} \frac{h_i}{\rho_i} \tag{7}$$

$$Ti = hi\rho i \tag{8}$$

Where,
S_i is the longitudinal resistance and T_i is transverse unit resistance,
and ρ_i and h_i are electrical resistivity and thickness of the *ith* layer respectively.

Table 1 *Aquifer protective capacity rating and vulnerability assessment [21]*

Rating	Remark
> 10	Excellent
5 to 10	Very good
0.2 to 4.9	Moderate
0.1 to 0.19	Weak
<0.1	Poor

3.2 Spatial Analysis

The inverse distance weighting (IDW) interpolation method in ArcGIS software (version 10.8.2) was used to graphically depict the groundwater pollutant concentration and spatial distribution in the study area. Furthermore, IDW is a kind of interpolation method that estimates unknown values at specified locations using known values at neighboring sites [22]. Equation (9) represents the IDW formula:

$$V = \frac{\sum_{i=1}^{n} \left(\frac{V_i}{d_i^p}\right)}{\sum_{i=1}^{n} \left(\frac{1}{d_i^p}\right)} \tag{9}$$

where p is a positive real number that controls the rate at which the weight decreases with distance, V is the estimated value at the target location, Vi is the known value at the ith known point, and
n is the total number of points used in the interpolation. di is the distance between the *ith* known point and the target location.

4. Results and Discussion

4.1 Geophysical Results

Tables 2 and 3 display the measured lithologies, thicknesses, depths, and apparent resistivities for ten (10) VES stations in the study area. The VES curves are created by plotting the apparent resistivity (ρa) on a bi-logarithm graph against the matching half electrode separation (AB/2). First, partial curve matching was used to analyse the sounding curves, and WIN resist was used to invert them. Figure 6 displays 1D inversion curves of some VES locations. Top soil, clay-sandy, sand-clayey, weathered basement, and fresh basement are the five geoelectric layers identified in the area. The three curve types identified are HA curve type (4,6,7,8), H curve type (VES 10), and QH curve type (VES 1, 2,3,5, 9) respectively. Resistivity values for the top soil layer range between 82 to 987 Ωm, thickness from 0.1 to 1.6m, and depth of 0.1 to 1.6m. The second geoelectric layer is clay-sandy with values of 84Ωm to 389Ωm, thickness between 0.2m and 9.2m and depth ranges between 0.3m to 10.8m.

Table 2 *Showing VES 1 to VES 6*

AB/2 (m)	MN/2 (m)	Apparent Res.(Ωm). VES 1	Apparent Res.(Ωm). VES 2	Apparent Res.(Ωm). VES 3	Apparent Res.(Ωm). VES 4	Apparent Res.(Ωm) VES 5	Apparent Res.(Ωm) VES 6
1.00	0.5	396	412	302	413	84	121
2.00	0.5	497	391	353	401	71	94
3.00	0.5	423	302	412	310	60	93
5.00	0.5	216	210	219	222	40	80
6.00	0.5	92	144	161	211	36	72
6.00	1.0	92	120	159	181	26	60
8.00	1.0	87	92	110	155	15	53
10.00	1.0	67	61	70	124	12	50
10.00	2.5	32	59	50	120	12	49
15.00	2.5	52	24	26	104	13	32
20.00	2.5	55	25	28	103	17	38
25.00	2.5	59	26	35	93	20	38
30.00	2.5	75	30	30	87	28	43
35.00	2.5	88	35	33	173	31	47
40.00	2.5	105	41	81	130	42	53
40.00	7.5	124	43	78	130	45	53
50.00	7.5	222	53	85	48	46	42
60.00	7.5	254	60	76	17	48	41
70.00	7.5	243	71	74	33	62	82
80.00	7.5	478	82	91	37	71	38
90.00	7.5	444	95	105	40	70	37
100.0	7.5	441	109	236	56	65	39
120.0	7.5	94	115	210	71	64	41
140.0	7.5	-	-	-	-	-	-
160.0	7.5	-	-	-	-	-	-

Table 3 *Vertical electrical soundings VES 7 to VES 10*

AB/2 (m)	MN/2 (m)	Apparent Res.(Ωm). VES 7	Apparent Res.(Ωm). VES 8	Apparent Res.(Ωm). VES 9	Apparent Res.(Ωm) VES 1
1.00	0.5	100	372	92	71
2.00	0.5	123	251	80	50
3.00	0.5	48	111	77	17
5.00	0.5	34	136	99	25
6.00	0.5	44	125	137	23
6.00	1.0	38	93	135	25
8.00	1.0	32	68	116	25
10.00	1.0	88	52	105	18
10.00	2.5	42	59	105	19
15.00	2.5	54	56	87	21
20.00	2.5	66	59	104	29
25.00	2.5	79	70	91	35
30.00	2.5	85	71	63	38
35.00	2.5	89	91	133	45
40.00	2.5	114	111	124	56
40.00	7.5	141	100	114	67
50.00	7.5	152	101	86	90

AB/2 (m)	MN/2 (m)	Apparent Res.(Ωm). VES 7	Apparent Res.(Ωm). VES 8	Apparent Res.(Ωm). VES 9	Apparent Res.(Ωm) VES 1
60.00	7.5	201	151	87	112
70.00	7.5	244	174	91	125
80.00	7.5	266	169	100	144
90.00	7.5	308	202	120	172
100.0	7.5	601	199	106	187
120.0	7.5	402	140	115	239
140.0	7.5	547	118	124	314
160.0	7.5	520	214	137	341

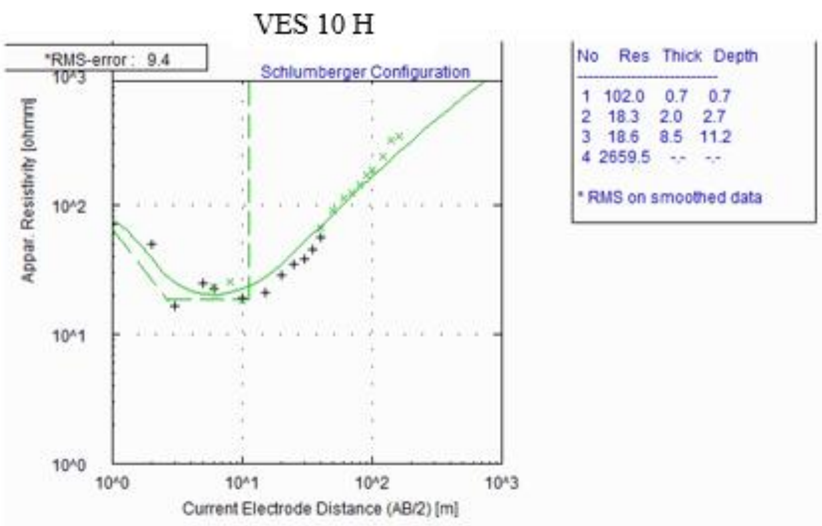

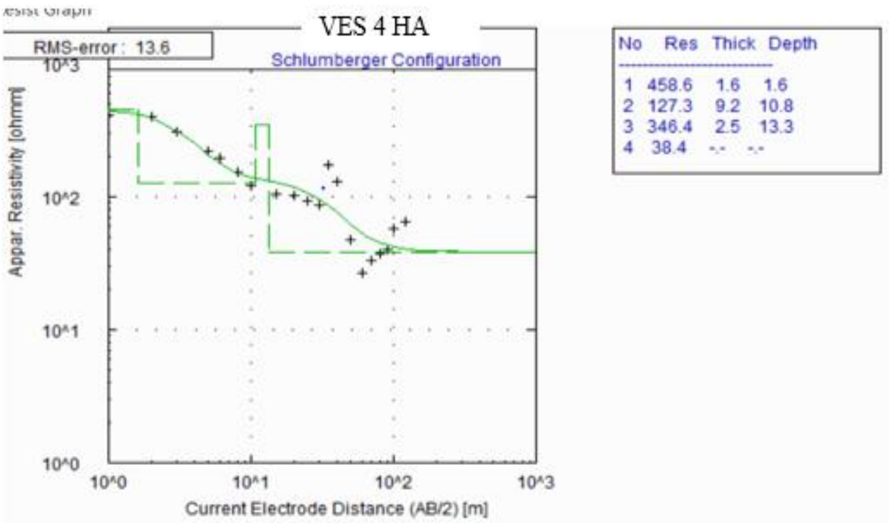

J. of Sustainable Natural Resources Vol. 7 No. 1 (2026) p. 34-46

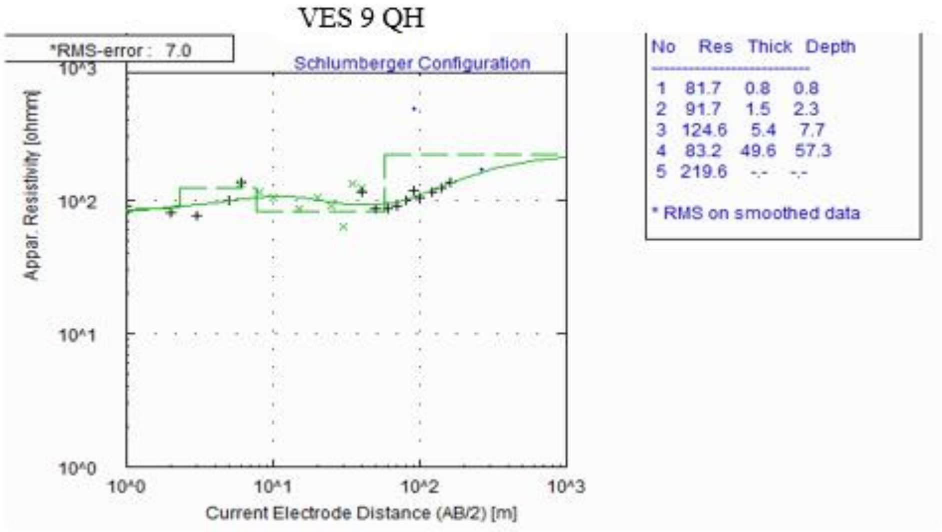

Fig. 6 *1D inversion curves of selected locations (VES 10, 4, and 9)*

Third geoelectric layer is sand-clayey with values ranges between of 18Ωm to 125Ωm, thickness of 2m to 6.2m and depth between 2.7m to 9.6m, fourth geoelectric layer is weathered basement with values ranges between 19Ωm and 1145Ωm, thickness of 0.5m to 50m and depth of 0.8m to 57.3m while the fifth geoelectric layer is fresh basement with values ranges between 34Ωm to 2847Ωm. The Isopach overburden and weathered basement maps (Figures 7 and 8) show that the area is covered by relatively shallow overburden in the north-west, south-west with thick overburden thickness in the south-eastern part. The underlying basement isoresistivity map (Figure 9) indicates that north-western and south-eastern regions have higher resistivity values, whereas the north-eastern, south, and south-western regions have lower resistivity values.

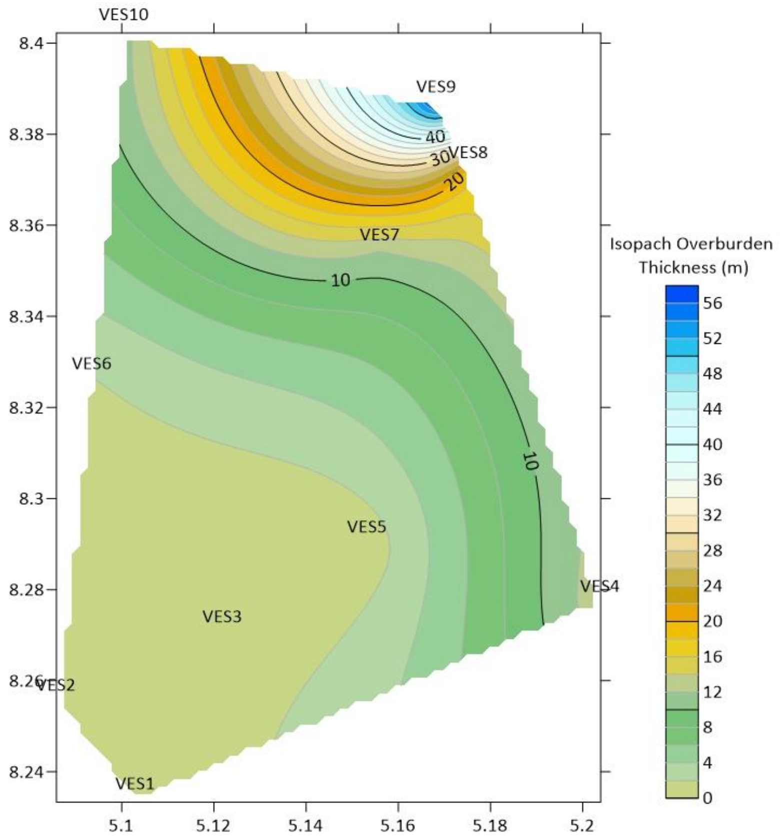

Fig. 7 *Isopach map of overburden thickness in study area*

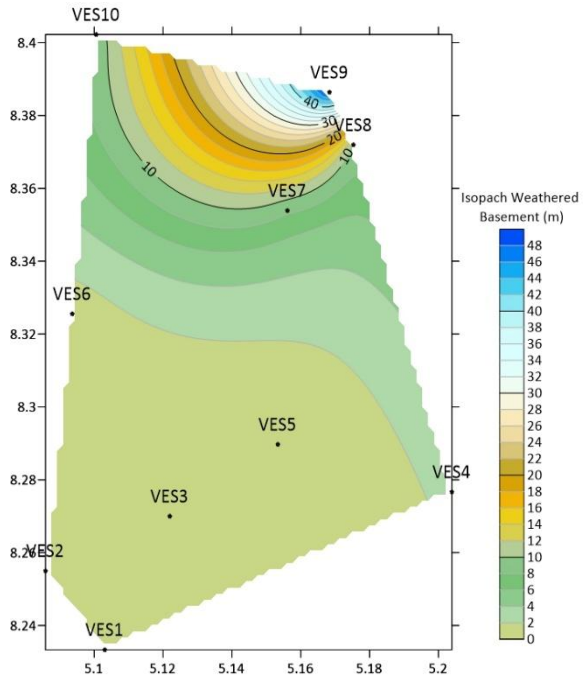

Fig. 8 *Isopach map of weathered basement in study area*

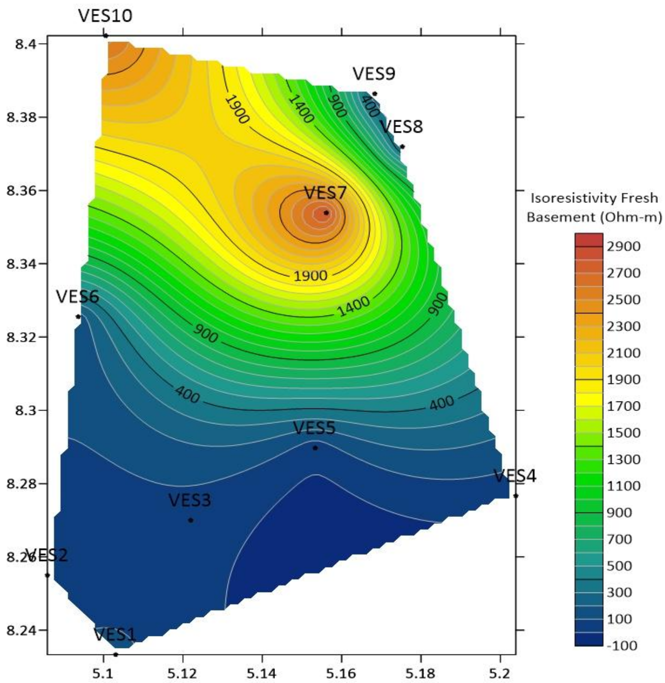

Fig. 9 *Isoresistivity map of fresh basement in study area*

4.2 Aquifer Protective Capacity and Spatial Distribution of Groundwater Vulnerability to Pollution in Study Area

The aquifer protective capacity of the study area is presented in Table 4. The rating was assigned and estimated aquifer protective capacity revealed that study area has aquifer protective capacity values ranges between 0.00 to 0.69 with a moderate zone (30%), weak zone (10%) and poor zone (60%). The moderate zones have values ranges from 0.23 to 0.69 and cover the northern to eastern parts of the area. The weak zone has value of 0.17, covering a few eastern parts of the area while poor zones are situated in the western to southern parts with values ranges between 0.00 to 0.01. Spatial distribution of groundwater vulnerability map for the area was generated using ArcGIS software (version 10.8.2) that shows different vulnerability zones (Figure 10). The grey colour shows area with moderate vulnerability, weak vulnerability zone is indicated by yellow colour while poor vulnerability zone is represented by the blue colour which covers most parts of the area and characterised with sandy-clay soils having 35% or more of clay and 45% or more of sand.

Table 4 *Aquifer protective capacity of study area*

Location	Aquifer Thickness (m)	Aquifer Resistivity (Ωm)	Aquifer Protective Capacity	Rating
1	0.8	1145	0.0007	Poor
2	1.7	683	0.0025	Poor
3	1.3	861	0.0015	Poor
4	13.3	346	0.0384	Poor
5	0.9	122	0.0073	Poor
6	1.9	144	0.0131	Poor
7	11.7	50	0.2341	Moderate
8	19.2	110	0.1745	Weak
9	57.3	83	0.6904	Moderate
10	11.2	19	0.5895	Moderate

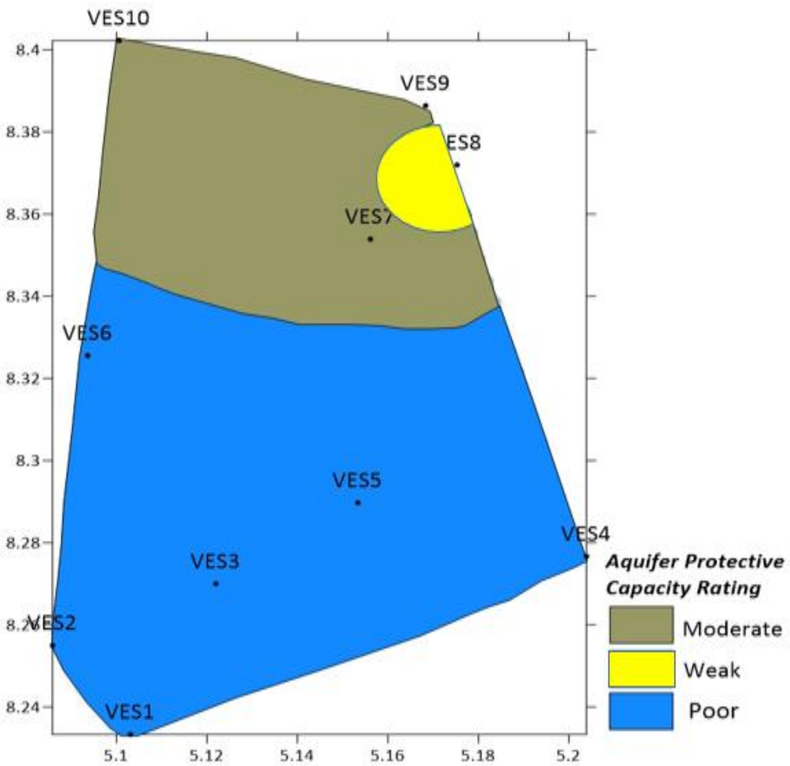

Fig.10 *Spatial distribution of groundwater vulnerability to pollution in study area*

5. Conclusion and Recommendations

This study has provided a spatially explicit framework for groundwater vulnerability assessment. The geophysical data shows that the study area consist mostly of clay-sandy soils with 35% or more of clay and 45% or more of sands. The study indicates that groundwater vulnerability in study area falls between moderate zone (30%), weak zone (10%) and poor zone (60%) thus indicating a poorly protected surface layer. This study has proved that geophysical method and GIS technique are effective tools for assessing and analysing groundwater vulnerability. Other methods of groundwater vulnerability assessments such as GOD, AVI and DRASTIC methods are recommended to complement the results of geophysical study. This study further recommended continuous monitoring of groundwater and controlling of mining activities to prevent further groundwater contamination in the study area.

Acknowledgement

The authors would like to thank all parties that have contributed towards the success of the study.

Conflict of Interest

Authors declare that there is no conflict of interests regarding the publication of the paper.

Author Contribution

The authors confirm contribution to the paper as follows: ***study conception and design:*** *Kehinde Olojoku Ibrahim, Rukayat Tolulope Ayanlere, Umar Faruk Aliyu, Azeez Adewale Adejumo, Abdulwahid Kolawole Aweda;* ***data collection:*** *Kehinde Olojoku Ibrahim, Rukayat Tolulope Ayanlere, Umar Faruk Aliyu, Azeez Adewale Adejumo, Abdulwahid Kolawole Aweda;* ***analysis and interpretation of results:*** *Kehinde Olojoku Ibrahim, Rukayat Tolulope Ayanlere, Umar Faruk Aliyu, Azeez Adewale Adejumo, Abdulwahid Kolawole Aweda;* ***draft manuscript preparation:*** *Kehinde Olojoku Ibrahim, Rukayat Tolulope Ayanlere, Umar Faruk Aliyu, Azeez Adewale Adejumo, Abdulwahid Kolawole Aweda. All authors reviewed the results and approved the final version of the manuscript.*

References

[1] Lijuan, W., Yuezan, T., Bin, S., & Peigui, L. (2022). Environmental and health risk posed by heavy metal contamination of groundwater in the Sunan Coal Mine, China. *Toxics, 10*, 390

[2] Ibrahim, K.O., Haruna, K.A., Folorunsho, I.O., & Ibrahim-Alli, O.K. (2023). Groundwater exploration in rural part of Ilorin, Northcentral Nigeria using electrical resistivity method, *COOU Journal of Physical Sciences, 6*(1), 344 – 361.

[3] Kekwaru, M.M., Udom, G.J., & Nwankwoala, H.O. (2022). *Groundwater exploration and aquifer protective capacity mapping in parts of River State, using geo-electrical resistivity survey*. Refereed proceedings of the 57th Annual International Conference of Nigerian Mining and Geosciences, Port Harcourt, Nigeria, 245 – 251

[4] Adegbe, M., Ile, T.O., Simon, S.A., Orji-Chukwu, N.J., Waziri, H.S., & Abubakar, A.E. (2017). Analyzing the environmental impacts and potential health challenges resulting from artisanal gold mining in Shango area of Mina, North-central Nigeria. *Journal of Degraded and Mining Lands Management, 5*(2), 1055 - 1063

[5] Tella, A.A., & Danjibo, N.D. (2024). The environmental impact of mining activities in the local community: A structural equation modelling approach. *International Journal of Social Work, 11*(1), 44 – 53

[6] Ibrahim, K.O., Gomo, M., Oke, S.A., & Yusuf, M.A. (2017). Vulnerability assessment of shallow aquifer hand-dug wells in rural parts of Northern Nigeria using AVI and GOD methods. *The Pacific Journal of Science and Technology, 18*(1), 325 - 333

[7] Foster, S.S.D. (1987). *Fundamental concepts in aquifer vulnerability, pollution risk and protection strategy.* In: W. van Duijvenbooden and H.G. van Waegeningh (Eds). Vulnerability of Soil and Groundwater to Pollutants, Proceedings and Information. TNO Committee on Hydrological Research. The Hague, 38, 69 – 78

[8] Van Stempvoort, D., Ewert, L. & Wassenar, L. (1993). Aquifer vulnerability index: A GIS comparative method for groundwater vulnerability mapping. *Canadian Water Resources Journal, 18*, 25 – 37

[9] Aller, L., Bennett, T., Lehr, J., Petty, R. & Hackett, G. (1987). *DRASTIC: A standard system for evaluating groundwater pollution potential using hydrologic settings*. National Water Association: Dublin, Ohio and Environmental Protection Agency: Ada, OK. EPA – 600 / 2- 87 – 035

[10] Civita, M. & De Maio, M. (2000). SINTACS R5 *A new parameter system for the assessment and authentic mapping of groundwater vulnerability to contamination*. Publ. No. 2200 del GNDC1 – CNR Pitagora Editrice: Bologna, Italy. 240

[11] Nwankwoala, H.O., & Udom, G.J. (2011). Hydrogeochemical evaluation of groundwater in parts of eastern Niger-Delta. *Journal of Academic and Applied Studies, 1*(2), 33 – 58

[12] Nwankwoala, H.O., Kekwaru, & M.M. (2019). Delineation of lithology and depth to groundwater using geo-electrical resistivity survey in Ndele Community, Rivers State, Nigeria. *American – Eurasian Journal of Scientific Research, 14*(4), 77 – 83

[13] Adedoyin, A.D., Ojo, O.J., Adekeye, J.I.D., & Alebiosu, M.T. (2020). Geochemical assessments of Owa-Kajola marble, South-western Nigeria. *NSUK Journal of Science and Technology, 7*(1), 89 – 93

[14] Ibrahim, K.O., Oke, S.A., Yusuf, M.A., & Purchase, M.W. (2024). *Health risk assessment of trace elements in groundwater around marble mine in Southwestern Nigeria.* Proceedings of the Faculty of Physical Sciences Conference, 26 -32

[15] Ejepu, J.S., Jimoh, M.O., Abdullahi, S., Abdulfatai, I.A., Musa, S.T. & George, N.J. (2024). Geoelectric analysis for groundwater potential assessment and aquifer protection in a part of Shango, Northcentral Nigeria. *Discover Water, 4*,33, 2004

[16] Bayewu, O.O., Oloruntola, M.O., Mosuro, G.O., Laniyan, T.A., Ariyo, S.O. & Fatoba, J.O. (2018). Assessment of groundwater prospect and aquifer protective capacity using resistivity method in Olabisi Onabanjo University Campus, Ago-Iwoye, Southwestern Nigeria. *NRIAG Journal of Astronomy and Geophysics, 7*(2), 347 – 360

[17] Alabi, O.O., Adeolu, O., & Akinpelu, D.F. (2016). Geophysical investigation for groundwater potential and aquifer protective capacity around Osun State University (UNIOSUN) College of Health Sciences. *Arabian Journal of Water Resources, 4*(6), 137 – 143

[18] Maillet, R. (1947). The fundamental equations of electrical prospecting. *Geophysics, 12*(4), 529-556

[19] Ehirim, C. Nwankwo, C. (2010). Evaluation of aquifer characteristics and groundwater quality using geoelectric method in Choba, Porth Harcourt. *Archives of Applied Science Research, 2*(2), 396 - 403

[20] Yusuf, S.N., Ishaku, J.M., Wakili, W.M. (2021). Estimation of Dar Zarrouk parameters and delineation of groundwater potential zones in Karlahi, part of Adamawa Massif, Northeastern Nigeria. *Water Geology, 47*(2), 103 – 112.

[21] Atakpo, E.A., & Ayolabi, E.A. (2009). Evaluation of aquifer vulnerability and the protective capacity in some oil producing communities of Western Niger-Delta. *The Environmentalist, 29*(3), 310 – 317

[22] Maleky, S., & Faraji, M. (2023). BTEX in ambient air of Zarand, the Industrial city in southeast of Iran: concentrations, spatial-temporal variation and health risk assessment. *Bulletin of Environmental Contamination and Toxicology, 111*(2), 25